# Green Chemistry

Accepted Manuscript






ROYAL SOCIETY OF CHEMISTRY

www.rsc.org/greenchem

Green Chemistry

ARTICLE

# Techno-Economic Analysis of a Conceptual Biofuel Production Process from Bioethylene Produced by Photosynthetic Recombinant Cyanobacteria

Received 00th January 20xx,
Accepted 00th January 20xx

DOI: 10.1039/x0xx00000x

www.rsc.org/

Jennifer N. Markham,[a] Ling Tao,[a]* Ryan Davis,[a] Nina Voulis,[b] Largus T. Angenent,[b] Justin Ungerer[a] and Jianping Yu[a]

Ethylene is the petrochemical produced at largest volume worldwide. It serves as a building block for a wide variety of plastics, textiles, and chemicals, and can be converted into liquid transportation fuels. There is great interest in developing technologies that produce ethylene from renewable resources, such as biologically derived $CO_2$ and biomass. One of the metabolic pathways used by microbes to produce ethylene is via an ethylene-forming enzyme (EFE). By expressing a bacterial EFE gene in a cyanobacterium, ethylene has been produced through photosynthetic carbon fixation. Here, we present a conceptual design and techno-economic analysis of a process for biofuel production based on upgrading of ethylene generated by the recombinant cyanobacterium. This analysis focuses on potential near-term to long-term cost projections for the integrated process of renewable fuels derived from ethylene. The cost projections are important in showing the potential of this technology and determining research thrusts needed to reach target goals. The base case for this analysis is a midterm projection using tubular photobioreactors for cyanobacterial growth and ethylene production, cryogenic distillation for ethylene separation and purification, a two-step Ziegler oligomerization process with subsequent hydrotreating and upgrading for fuel production, and a wastewater treatment process that utilizes anaerobic digestion of cyanobacterial biomass. The minimum fuel selling price (MFSP) for the midterm projection is $15.07/gallon gasoline equivalent (GGE). Near-term and long-term projections are $28.66/GGE and $5.36/GGE, respectively. Single- and multi-point sensitivity analyses are conducted to determine the relative effect that chosen variables could have on the overall costs. This analysis identifies several key variables for improving the overall process economics and outlines strategies to guide future research directions. The productivity of ethylene has the largest effect on cost and is calculated based on a number of variables that are incorporated into this cost model (i.e., quantum requirement, photon transmission efficiency, and the percent of energy going to either ethylene or cyanobacteria biomass production).

## 1. Introduction

Ethylene is the petrochemical produced at largest volume worldwide, and it is used for more than 50% of the total polymer production by volume, making it one of the most used chemicals for the industrial world.[1,2] Because the ethylene market is so large, with a production capacity of 120 million (MM) metric tons in 2010, it is often used as a proxy for the chemical industry's performance as a whole.[3,4] In addition to polymer production, ethylene is a building block for many other chemicals and can also be upgraded into gasoline, diesel, and jet fuels.[5]

Before World War II, ethylene was produced from the dehydration of ethanol, but that process was partially replaced with the advent of cheaper fossil feedstocks.[1] Today, nearly all ethylene is produced from fossil sources, primarily through steam cracking of naphtha, gasoil, and condensates.[1,2,4] In recent years, a commercial bioethylene plant has started operation. Brazil-based Braskem has been making bio-polyethylene since 2010 with an annual capacity of 180,000 metric tons.[6] Braskem produces ethylene through a sugar-to-ethanol-to-ethylene pathway that utilizes sugarcane grown on arable land.[6] With the knowledge that (1) fossil sources are finite; (2) the cost of fossil feedstocks continues to vary; and (3) the conventional steam-cracking process produces greenhouse gases (1.5–3.0 tons of $CO_2$ per ton of ethylene), it is clear that renewable bioethylene should be considered as an addition or replacement to the petroleum-dominated ethylene market.[1,3]

Besides catalytic conversion from bioethanol, ethylene can be biologically produced by plants, bacteria, and fungi.[7-9] National Renewable Energy Laboratory (NREL) and others have developed the cyanobacterium *Synechocystis sp.* PCC 6803 (henceforth referred to as *Synechocystis*) that produces ethylene via photosynthetic carbon assimilation.[3] As plants use ethylene to regulate germination, senescence, and fruit ripening, plant pathogens have developed pathways to produce ethylene to weaken their hosts.[3] One of these pathways uses the ethylene-forming enzyme to catalyze a single-step reaction involving components of the tricarboxylic acid cycle (TCA cycle).[3] This pathway, when compared to other bio- and fossil-based alternatives for ethylene production, holds great potential for commercial applications. Ethylene can be produced on non-arable land with this pathway. The recombinant *Synechocystis* can also use biomass sugars as a supplemental energy source to enhance ethylene productivity when sunlight is not present or sufficient.[10] Additionally, *Synechocystis* can be grown in saline or brackish water.

[a] National Renewable Energy Laboratory, 15013 Denver West Parkway, Golden, CO 80401
[b] Cornell University, Biological and Environmental Engineering, 226 Riley Robb Hall, Ithaca, NY 14853-5701
* Corresponding Author Email: Ling.Tao@nrel.gov, Tel: 1-303-384-7809

### 1.1. Previous Bioethylene Production Pathways and Research

There are three pathways for ethylene production in plants, bacteria, and fungi. In the plant pathway, ethylene is generated by a two-step mechanism where methionine is incorporated into S-adenosyl-methionine (SAM) that is first converted to 1-aminocyclopropane-1-carboxylic acid (ACC), which is then reduced to ethylene and cyanide.[11] A second pathway utilized by microbes consists of the oxidation of 2-keto-4-methylthiobutyric acid to ethylene, which produces only trace amounts.[11] A third pathway, found in certain fungi and bacteria, produces ethylene via the ethylene-forming enzyme (EFE). Knowledge of EFE reaction is incomplete; the reaction formula and mechanism is currently under investigation. Fukuda et al.[12] proposed that EFE reaction follows the equation shown below, with AKG standing for alpha-ketoglutarate and P5C standing for 1-pyrroline-5-carboxylate:

$$3\,AKG + 3O_2 + L-arginine \rightarrow 2\,ethylene + succinate + 7CO_2 + guanidine + P5C \qquad \text{(Equation 1)}$$

NREL's recombinant *Synechocystis* produces ethylene by EFE from the bacterium *Pseudomonas syringae*.[3] Figure 1 shows the metabolic pathway utilized by the recombinant cyanobacterium and possible areas of future research that could lead to higher productivity of ethylene, thus potentially reaching the target levels described in this paper. The NREL recombinant *Synechocystis* produces ethylene photosynthetically with a maximum demonstrated productivity of 739 mg/L/day at the bench scale[13] and also enhanced photosynthetic activities including carbon fixation, oxygen evolution rates, and increased carbon flux through the TCA cycle.[14] Ethylene, as a gas, diffuses out of the medium and circumvents issues related to liquid-liquid product separation of the medium and the product.[3] Ethylene is non-toxic to the cells.

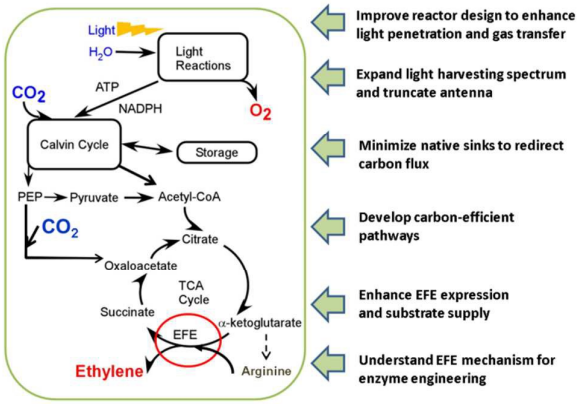


**Figure 1. Metabolic pathways in *Synechocystis* leading to ethylene production and proposed future research areas toward higher productivity.**

### 1.2. Other Products Produced from Photosynthetic Algae and Cyanobacteria

Algae have been commercially cultivated for human consumption, animal feed, and production of pigments and pharmaceutical products since the 1960s.[15] Additionally, algae have been identified as potential feedstocks for hydrocarbon (HC) biofuels. Many of the products produced by wild-type algae are contained within the cell. Thus, to harvest the product the whole algal biomass needs to be harvested. On the other hand, genetically tractable cyanobacteria strains have been engineered (recently reviewed in Angermayer et. al,[16] and Lai and Lan[17]) to secrete target products. The supplementary information tables S1 and S2 provide a review of algae products and secreted products from cyanobacteria. Ethylene productivities are among the highest in mass or moles of carbon at 739 mg/L/day and 52.7 mmol of fixed carbon/L/day.

Ethylene has other benefits that lend it to being the topic for cost analysis. Similar to isoprene and hydrogen, ethylene is not toxic to *Synechocystis* and is secreted into the headspace of a closed cultivation system, the photobioreactor (PBR), as a gas. The generation of secreted products provides an added benefit because neither carbon flux nor the enzymatic reaction is limited or slowed down by product accumulation; to the contrary, carbon fixation is stimulated by ethylene production.[14]

Quantum requirement is a method of describing the stoichiometric constraints for the photosynthetic reaction mechanism to products. Unlike other products that have well defined reaction mechanisms and quantum requirements, ethylene's reaction mechanism using the EFE gene is incomplete and literature values for the ethylene quantum requirement vary. A literature search for the quantum requirement for ethylene produces a range of values: 24 mol photons/mol ethylene (equivalent to 12 mol photons/mol $CO_2$),[18] 36 mol photons/mol ethylene,[19] 44 mol photons/mol ethylene,[20] 48 mol photons/mol ethylene,[21] 61 mol photons/mol ethylene.[20,22] These values suggest lower photon energy conversion efficiency compared to that of some other products (8-13 mol photons/mol product). This limitation is a major challenge for achieving high ethylene productivity. However, the actual productivities reported for generation of other products tend to be much lower, suggesting that factors other than quantum requirement play a major role in the overall product generation and, obviously, productivities depend on the light intensity used during cultivation.

### 1.3. Current Research Development on *Synechocystis* to Bioethylene

NREL has engineered genetically stable *Synechocystis* strains that convert $CO_2$ to ethylene from photosynthetically fixed carbon.[3] Ethylene productivity has been incrementally increased, through a series of genetic improvements, to reach a peak productivity rate of 30 mg/L/h in the laboratory. This rate was measured with a *Synechocystis* strain (*JU547*) that carries a single copy of *efe* gene per genome, and in which the EFE protein production was enhanced by the engineering of a synthetic ribosome-binding site.[14] The ethylene production rate was measured according to previously published work[3] but under light intensity of 1,500 µmol photon $m^{-2}$ $s^{-1}$. This light intensity is expected to be close to peak illumination inside a PBR exposed to sunlight. The amount of fixed $CO_2$ that is converted into ethylene is 10% when cells are cultivated to an $OD_{730}$ of 5.0, implying that 90% of the fixed carbon is used for cell biomass growth instead.[14]

The stability of photosynthetic ethylene production has also been evaluated by Cornell University using semi-batch cultures of a previously published 2x*efe* strain.[3] This 2X *efe* strain was generated earlier than *JU547* and did not benefit from the synthetic ribosome-binding site that was engineered into *JU547*. 2X*efe* was shown to direct 5.7% of its fixed carbon to ethylene production.[3] Ethylene production was maintained for 71 days, including 12 days of seeding time, until the experiment was arbitrarily terminated (Figure 2). The data demonstrated genetic stability of our ethylene producing strains. Based on data shown in Figure 2, turnover time



 

in the techno-economic analysis (TEA) is assumed to be 60 days for near-term target and 330 days for long-term targets.

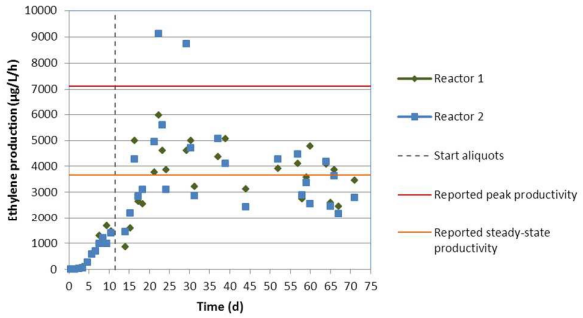


**Figure 2. Ethylene productivity by the 2X *efe* strain**over 72 days in duplicate semi-batch reactors. Experimental details are shown in the Supplementary Information. For reference, the published[3] peak production rate (7.125 mg/L/h) and steady-state production rate (3.660 mg/L/h) have been indicated by the solid red and orange lines.

Although there are several advantages to generating bioethylene from photosynthesis using *Synechocystis*, understanding the economic potential for the process at a commercial scale is critical to guide research and development towards viability of this technology. Indeed, rigorous cost analyses have yet to be made public and remain a key uncertainty for further development of this nascent technology. Ethylene, as a building block chemical, can be converted to chemicals or hydrocarbon fuels.[5] Converting ethylene to hydrocarbon fuel is a well-known commercial technology. The goal of this work is to perform a TEA to assess the economic potential of producing renewable fuels from a bioethylene-to-hydrocarbons pathway using solar insolation as the energy input, in order to guide research in the most beneficial direction. Use of biomass sugars as a supplemental energy input, or converting bioethylene intermediate to chemicals are possible, but are not included in this analysis and will be considered in future studies.

## 2. Materials and Methods

The TEA includes a conceptual process design, detailed process modeling for rigorous calculation of the material and energy balances using Aspen Plus, and translation of the resulting capital investment, project, and operating cost estimates into discounted cash flow calculations. From this information, a minimum GGE selling price was established based on a stipulated 10% internal rate of return, with a sensitivity analysis performed on key performance parameters.

### 2.1. Process Overview

The simplified process flow diagram shown in Figure 3 illustrates six main process function areas (Area 100 to Area 600), including cultivation systems for ethylene production (A100), ethylene purification (A200), ethylene catalytic upgrading to hydrocarbons (A300-400), on-site wastewater treatment (A500), and utilities including a cooling tower and refrigeration system (A600).

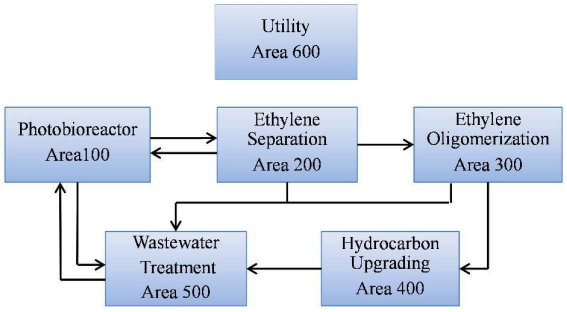


**Figure 3. Simplified process block flow diagram.**

**2.1.1. Area 100 Photobioreactor.** In this design, closed cultivation systems are utilized to produce ethylene and biomass in a process similar to that used for algal biomass cultivation. This area includes a closed cultivation system inoculated with seed cell culture for cyanobacteria growth and ethylene production, with adequate solar radiation to achieve the targeted productivity values. An assumed ethylene production of 7.2 g/m$^2$/d is used for our base case cost analysis. This value is calculated using the approach by Weyer et al.[23] and is based on physical laws, an assumed value of quantum requirement, and a location that has an annual solar irradiation of 6,000 MJ/m$^2$/year (see supplementary information table SI3 for example locations and their associated average solar irradiance).[24] Figure 4 and Table 1 show the assumptions used to reach the 7.2 g/m$^2$/day base value calculation. Sensitivity analyses are performed to determine the effect of different parameters on ethylene productivity.

Figure 4 and Table 1 show the critical assumptions for efficiencies that, when compounded, lead to a final percent of total irradiance available for ethylene and biomass production. The most critical assumption in calculating ethylene productivity is the insolation value per year, which is set at 6,000 MJ/m$^2$/year (assumption 1).[23] Of the full solar energy spectrum, 45.8% is photosynthetically active radiation (PAR) (assumption 2).[23] Ninety-five percent of photons are transmitted through an open pond.[23] Additionally, 90% of photons are assumed transmitted through the plastic of the PBR.[25] Once the photosynthetic portion of the sunlight reaches the PBR cultivation system, only 86% is transmitted through the plastic cover and absorbed by the media, the rest is reflected by the surface (assumption 3).

Under sub-optimal cultivation conditions, the photon utilization efficiency, which is the cyanobacteria cell's ability to absorb available photons, ranges from 10% to 30% under high light, or 50% to 90% under low light conditions. Sub-optimal condition photon losses can be due primarily to photoinhibition, the low light-saturation of photosynthesis, and non-optimal cultivation parameters. Therefore, consistent with Weyer et al.[23] we assume a median value of 50% for the photon utilization efficiency per year (assumption 4). This brings the "utilizable" energy to 1,182 PAR MJ/m$^2$/year.

The biomass and ethylene accumulation efficiency is the amount of energy that can be made available for biomass and ethylene accumulation while accounting for homeostasis ("cost of living") for the cell. The biomass and ethylene accumulation efficiency is set at 55% of the utilizable energy (assumption 5), and when it is accounted for, the total energy that is allocated to biomass and ethylene production is 650 PAR MJ/m$^2$/year or 10.8%

of the incident radiation. Similarly, Weyer et al.[23] presented 10.8% of the total energy being utilized for biomass production.

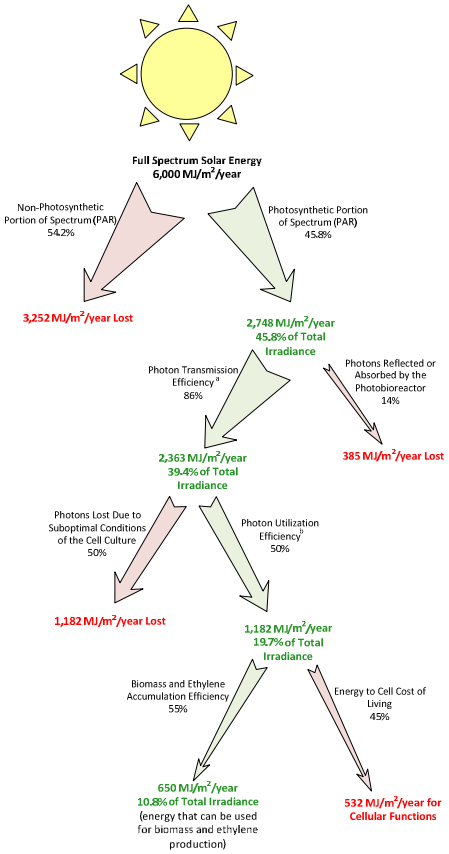


**Figure 4. Solar energy losses and uses.** [a] Photon transmission efficiency accounts for light reflection or absorption by the surface and material of the cultivation system. [b] The photon transmission efficiency relates to the percent of photons that are transmitted through the closed pond liners into the media.

The biomass accumulation efficiency was increased from 50%[23] to 55% to compensate for the reduction in photon transmission efficiency from 95%[23] to 86% in order to reach the same 10.8% energy to products. Given that there is a wide range of the biomass accumulation efficiency from 35% to 89%,[23] the 55% assumption is reasonable. To make sure that the theorized ethylene productivity does not reach unreasonably high levels, this 10.8% percent of energy to products was set as the base case constraint. During the sensitivity analysis for future research described in section 3.2.4 the 11% constraint is increased to 16%, which increases the biomass and ethylene accumulation efficiency to more than 75%. Finally, we set a target of 78% conversion of this energy into ethylene (assumption 6), and 22% into biomass (assumption 7), giving a base case with solar energy that can be converted into ethylene at 8.3% of the incident sunlight.

The conversion of light energy into chemical energy is further impacted by the quantum requirement to create the product. For biomass growth from carbohydrates, eight photons are required to make one $CH_2O$ carbohydrate unit via photosynthesis. The energy contained within the carbohydrate unit is less than the energy needed to create it.[23] The mechanism pathway creates stoichiometric constraints on the maximum product yield per unit energy for ethylene and biomass. This maximum yield determines the quantum requirement.

**Table 1. Ethylene Productivity Assumptions for the Base Case.**

| Assumptions | Base Case |
|---|---|
| 1. Full Spectrum Solar Energy (MJ/m$^2$/year) | 6,000 |
| 2. Photosynthetic Portion of Spectrum (PAR) | 45.80%[23] |
| 3. Photon Transmission Efficiency | 86%[a] of PAR[23,25] |
| 4. Photon Utilization Efficiency | 50% of PAR photons transmitted into the closed ponds[23] |
| 5. Biomass Accumulation Efficiency | 55%[b, 23] |
| **Total Energy Going to Biomass and Ethylene Production (MJ/m$^2$-year)** | **650** |
| **Percent of Total Irradiance Going to Biomass and Ethylene Production** | **10.8%** |
| 6. Energy Partitioning for Ethylene Production | 78%[c] (8.4% of total irradiance) |
| 7. Energy Partitioning for Biomass Production | 22% (2.4% of total irradiance) |
| 8. Photon Energy of PAR (MJ/mol) | 0.2253[23] |
| 9. Quantum Requirement Ethylene (Biomass) | 24 mol photons/mol ethylene (8 mol photons/$CO_2$ to biomass)[18,23] |
| 10. Ethylene Energy Content LHV (MJ/kg) (Biomass Energy Content (MJ/kg)) | 47.2 (21.9)[23] |
| **Calculated Productivities and Efficiencies** | |
| Ethylene Productivity (g/m$^2$/day) | 7.2[d] |
| Cyanobacteria Biomass Productivity (g/m$^2$/day) | 5.1 |
| Overall Energy Efficiency for Ethylene and Biomass (energy content of product/total sunlight) | 2.8% |
| Ethylene Overall Energy Efficiency | 2.1% |
| Biomass Overall Energy Efficiency | 0.7% |

a. Photon transmission efficiency accounts for light reflection or absorption by the surface and material of the cultivation system. Ninety-five percent of photons are transmitted through an open pond.[23] Additionally, 90% of photons are assumed transmitted through the plastic of the PBR.[25] Thus, 86% of photons are transmitted to the media.

b. Biomass accumulation efficiency is set 5% higher than the same assumption in the Weyer et al. paper to allow for percent of total irradiance used for biomass and ethylene production to match the Weyer et al. paper.

c. Energy partitioning to ethylene is the percent of energy that goes to ethylene creation out of the 10.8% of the total solar irradiance that is available for ethylene and biomass production.

d. This productivity value is projected for research and has not been demonstrated in the laboratory.

Although the quantum requirement for the ethylene-forming enzyme pathway is still to be determined, a value of 12 mol photons/mol $CO_2$ (equivalent to 24 mol photons/mol ethylene)[18] was chosen to represent the base case scenario. This value assumes that the other products of the pathway, such as guanidine, are reintegrated into the cell and metabolized. When no coproducts are reintegrated to the cell the quantum requirement is much higher at 30.5 mol photons/mol $CO_2$ (equivalent to 61 mol photons/mol ethylene).[20] A quantum requirement of 8 mol photons/mol $CO_2$ reduced to biomass is also considered. The 10.8% of the incident sunlight energy accumulated into ethylene and biomass is converted into moles of photons per area, as per Weyer et al.,[23] assuming a value of 0.2253 MJ/mol for an average 531 nm-photon, yielding a photon flux density for product creation of 2,885 PAR mol photons/m$^2$ year (2,250 PAR mol photons/m$^2$ year for ethylene production and 635 PAR mol photons/m$^2$ year for biomass

production). Using the quantum requirement and the molecular weight of ethylene, the productivity of ethylene for the base case is set to 7.2 g/m$^2$/day after being normalized to a daily production rate, as shown in Table 1. The overall energy efficiency is the amount of energy contained within the products divided by the full spectrum solar energy. For a productivity of 7.2 g/m$^2$/day, 124 MJ/m$^2$/year of energy is contained in the ethylene, giving an overall energy efficiency of 2.1% (130 MJ/m$^2$/year energy in the ethylene / 6,000 MJ/m$^2$/year), and a photosynthetic efficiency of 4.7%. Note that this is not a theoretical maximum of ethylene productivity but a midterm projection case that may be achievable through research and development. Improving the ethylene productivity beyond 7.2 g/m$^2$/day may also be possible as discussed in the sensitivity analysis section, including both more near-term and long-term research projections.The assumed cyanobacteria elemental formula is set as $C_{100}H_{162}O_{40}N_{22}P$ from literature.[26] The molar balance of carbon dioxide and water needed for ethylene is formulated as $2CO_2 + 2H_2O \rightarrow Ethylene + 3O_2$,[3] although it clearly does not reflect the actual reaction. This elemental formula is also used to determine the required nutrients such as ammonia and diammonium phosphate for biomass nitrogen and phosphorous respectively.

There are multiple options for photosynthesis reactors in literature for algae production.[27] Because ethylene is collected from the gas phase of a photosynthesis reactor, a closed system is required. A system of rigid tubular PBRs is considered as the base case. The PBR is comprised of horizontal tubes with an inner diameter of 8 cm and 80 m long sections, as described by Davis et al.[28] The headspace accounts for 20% of the reactor volume in this design. For the sensitivity analysis, a cultivation of covered ponds is considered. The covered ponds are covered with low-density polyethylene operating at 20-cm liquid depth.[28-31] The design and cost details for the pond match the information present in Lundquist et al.[30] The areal productivity per square meter of 7.2 g/m$^2$/day from Table 1 is set the same for both the covered pond and the PBR system. For the PBR, 200 m$^3$ of PBR tubes (250 m$^3$ of PBR plus headspace) covers one hectare of land, based on existing literature.[28] Table 2 shows the areal productivity for covered ponds and the corresponding volumetric productivity for PBRs. In either case, the design basis is set to produce ethylene that can be upgraded to 10 MMGGE hydrocarbons per year. The areal productivity is the same for both cases and this translates to the same facility size for the cultivation area. By having the same areal productivity, the two cases will invariably have different volumetric productivities as they have different volumes. The total footprint accounts for all processing operations, and additional piping. Unlike other TEA models that plan the full layout,[30-32] the cultivation area is set as 84% of the total area of the facility, similar to other designs.[32] The base case plant total footprint is 3,635 acres, of which 3,053 is the area for PBRs (known as the cultivation area), shown in Table 2.

The $CO_2$ delivered to the cultivation systems is assumed to be sourced from off-site power plant flue gas carbon capture technologies to yield concentrated $CO_2$, with the cost for flue gas carbon capture and delivery estimated at $40/metric ton.[28] The $CO_2$ is bubbled and directly injected into the covered ponds and PBR, respectively. It is assumed that the cultivation reactors achieve a 90% $CO_2$ retention going to ethylene and biomass with 10% contained in headspace gasses.[32] The PBR uses airlift column degassing stations to strip and remove the gas phase. The closed pond requires compressors to remove the headspace gases (one compressor per hectare). The gas mixture is sent to Area 200 to recover ethylene. Separated $CO_2$ is recycled back to either covered ponds or PBRs.

**Table 2. Productivity Baseline Assumptions.**

| | PBR | Covered Pond (Sensitivity) |
|---|---|---|
| Scale (MMGGE/yr) | 10 | 10 |
| Facility size (acres; cultivation PBR only) | 3,053 | 3,053 |
| Total Footprint (acres; includes processing, storage, etc.) | 3,635 | 3,635 |
| Ethylene Productivity | 7.2 g/m$^2$/day (359 mg/L/day) | 7.2 g/m$^2$/day |
| Biomass Productivity | 5.1 g/m$^2$/day (257 mg/L/day) | 5.1 g/m$^2$/day |

Both the closed pond and PBR reactors are closed systems with no evaporative losses. Instead of the evaporative cooling possible with open ponds, these reactors need additional cooling.[33] The PBR assumes a sprinkler system for cooling, whereas the covered pond uses a cooling tower system. The amount of heat the cooling tower removes from the closed ponds is based on temperature modeling of a closed PBR in literature.[33] The cyanobacteria are grown at 30°C–40°C[14] and 32 GJ/ha/day are calculated to be absorbed by the closed ponds at that production temperature.[33]

The cultivation systems are assumed to run on a continuous basis with the off-gasses being removed continuously. The culture in each closed pond is assumed to be purged every 60 days (turnover time) and the cyanobacteria biomass, water, and other nutrients are sent to the wastewater treatment (WWT) area (Area 500), which contains an anaerobic digestion system, a gas turbine on the biogas line; the nutrients and water are then recycled back to the closed cultivation system. The purge basis means that in any one day 2% of the cultivation systems are being purged and re-inoculated. Substantial fractions of $CO_2$, nutrients, and water are recycled from the WWT and ethylene separation and purification operations (Area 200), and make-up rates are subsequently calculated to close mass balances.

**2.1.2. Area 200 Ethylene Separation.** The gas phase from the cultivation systems containing ethylene, unconverted $CO_2$, oxygen, and water vapor is sent to Area 200 to undergo ethylene separation. Although the presence of $CO_2$ does not affect the oligomerization of ethylene, larger reactors would be needed for this operation. Oxygen and ethylene are reactive at concentrations ranging from 2.7 vol% to 36 vol% ethylene,[34] and the ethylene must be separated from the oxygen before the catalytic reaction takes place. To stay outside the flammability zone, additional air is pumped into the covered ponds and PBRs to maintain the ethylene concentration below 2.7 vol%. This increases the energy requirement for separation, but reduces the risk of fire at the plant.

Ethylene purification technologies from light olefins in commercial operations include cryogenic separation, solid pressure swing adsorption, liquid absorption of ethylene with solvent recovery, and membrane separation.[35-38] Although many of these separation methods have been employed by the natural gas industry to capture methane and ethylene from other light hydrocarbons, there is little information on the effect of oxygen on the process esign. Two separation methods (cryogenic distillation and liquid absorption) are considered and compared in this study, allowing us to explore different separation technologies for

economics. Cryogenic distillation is a commercially proven technology for ethylene purification, but it could be potentially expensive due to the large power demand for cooling and compressing gas streams. Liquid absorption, on the other hand, can be more energy efficient, but it could require a capital-intensive design and its effectiveness in purifying ethylene from $CO_2$ and $O_2$ is not proven.

For the cryogenic separation approach, $CO_2$ is removed first by an amine-based system since $CO_2$ solidifies at the operating conditions for the process. Water vapor is removed by molecular sieves before the gas mixture is applied to the distillation column. An alternative approach involves applying a "Controlled Freezing Zone Process",[39] which utilizes cryogenic distillation columns designed to have a zone that allows for solids formation. In the liquid absorption separation method $CO_2$ is again first removed by an amine-based absorber and stripper. This reduces $CO_2$ build-up within the oligomerization reactor. Water is removed via a molecular sieve. Ethylene absorption using solvents has been extensively discussed in the patent literature.[40-44] Hydrocarbons that are created downstream in Areas 300 and 400 are used as a solvent to recover ethylene.[40] The off-gas is compressed and cooled to 10 bar and 15°C before entering the absorption column to recover a higher percentage of ethylene.[40] Paraffins in the $C_6$–$C_{10}$ range are sent to the absorption column at 10 bar and -22°C.[40] The on-site chilling requirement is supplied by a propylene refrigeration unit. Patent examples describe ethylene recovery reaching 99.16%.[40] The solvent flow into the absorber is determined by the model in order to recover nearly all of the ethylene in the gas. After absorption the ethylene-rich solvent is sent to a distillation column where the ethylene is recovered. The solvent is recycled to the absorber with a make-up solvent stream to account for lost solvent. For both cases, the purified ethylene stream is sent to Area 300 for oligomerization and $CO_2$ is recycled back to the cultivation system.

**2.1.3. Area 300 Ethylene Oligomerization.** Production of hydrocarbon fuel (gasoline and diesel) blendstocks via ethylene oligomerization is a process technology that has been known for more than 70 years.[5] It is a well-established process for which no further technological breakthroughs are expected, except improvements in catalyst design. Three commonly used commercial homogeneous technologies for ethylene oligomerization include the Ziegler one-step process used by Chevron Phillips (capacity 680,000 metric tons per year, 2002), the Ziegler two-step process utilized by the Ethyl Corporation (now Ineos, capacity 470,000 metric tons per year, 2002), and the Shell Higher Olefin Process (SHOP) developed by Shell Oil Company (capacity, 320,000 metric tons per year, 1977).[45,46] We consider the two-step Ziegler process here, with separate oligomerization and hydrogenation reactions. In the oligomerization reaction, ethylene is converted to linear α-olefins.

The catalysts used to initiate this reaction have been broadly studied and include the Ziegler type catalysts,[46] chromium-based catalysts,[47] and ligand catalysts using different metal bases such as nickel.[48,49] Commercial processes for ethylene oligomerization often use homogeneous catalysts to reach the lower density oligomers that are below 30 carbon chain lengths. For instance, the homogeneous Ziegler catalyst is used for two different processes including the single-step process used by Chevron Phillips and the two-step process used by Ineos.[2,45,46] The two-step Ziegler process regenerates the catalyst whereas the single-step process uses the transformed catalyst as a coproduct.[2,50] To reduce the number of coproducts formed in the process, the two-step Ziegler process was chosen for fuel production in this model. The reaction occurs in two reactors with the first for oligomer generation occurring at 90°C–120°C and 100 bar.[51] The second reactor displaces the oligomers attached to the triethylaluminum catalyst with ethylene at 200°C–300°C and 10 bar.[51] Based on similar processes from literature, such as the one-step Ziegler process[52] and other ethylene oligomerization commercial processes using homogeneous catalysts,[53] it was assumed that tubular reactors are used for this reaction system.

The reaction conditions and oligomer separation are further discussed in Lanier[50] and utilize tandem flash tanks and centrifugal separators. The final product distribution of olefins is 5% $C_4$, 10% $C_6$, 16% $C_8$, 19% $C_{10}$, 18% $C_{12}$, 15% $C_{14}$, 9% $C_{16}$, 5% $C_{18}$ , and 3% $C_{20\text{-}C20+}$.[51] The mix of olefins includes 95% linear alpha-olefins, 4% branched olefins, and 1% linear olefins that are not alpha-olefins.[51] The ethylene conversion is assumed to go to completion because the unreacted ethylene is recovered based on literature of similar reactions with ethylene recovery and recycle.[53] This study assumed the use of the oligomerization reaction catalyst (Ziegler) with a calculated weight hourly space velocity (WHSV) of 2 $h^{-1}$ based on literature data,[50] a density of 836 kg/$m^3$ (52.19 lb/$ft^3$) at 20°C,[54] and a cost of $6.04/kg ($2.74/lb)[55] with annual replacement. Make-up catalyst is also considered for the lost catalyst contained in a purge stream. In order to reduce build-up of mid-range olefins, a purge stream is included. Similar to other designs, the total amount of product purged is equal to 5% by weight of the aluminium content of the stream going to the displacement reactor.[50]

A hydrotreating reactor is used to saturate the olefins to alkanes. Two common catalysts for this are cobalt molybdenum (CoMo)[56] and palladium or platinum (Pd or Pt) on activated carbon.[57] This study assumed that the CoMo catalyst is used with a WHSV of 3 $h^{-1}$.[56,58] The yield is assumed 100% to alkanes at 370°C[56] and 35 atm.[59] After hydrotreating, a hydroisomerization step is applied to convert normal paraffin to their isomers. The bi-functional catalysts used for isomerization contain platinum-containing zeolite catalysts at 1 $h^{-1}$ WHSV in the 250°C fixed bed reactor similar to the hydrotreating step.[60-63] Hydroisomerization catalyst life is usually three years or more, and an atmosphere of hydrogen is used to minimize carbon deposits on the catalyst but hydrogen consumption is negligible.[61]

**2.1.4. Area 400 Hydrocarbon Fractionating.** A series of distillation columns are used to fractionate hydrocarbons into gasoline, diesel, and jet fuel blendstocks. The light paraffins are $C_2$–$C_4$ hydrocarbons that can be recycled back to the oligomerization reactor or sent to a combustor. In this model, this stream is sent to the combustor. The product cut containing $C_5$–$C_8$ components constitutes gasoline-range fuel. Carbon numbers in the range $C_9$–$C_{16}$ are considered to be jet-range blendstocks. All products having carbon numbers higher than $C_{16}$ are considered diesel blendstocks. However, engine testing and quantification of fuel properties for each product cut (e.g., octane number, vapor pressure, cetane number, and cloud point) would be required to fully understand each product's suitability for fuel blendstock purposes. For the purpose of overall hydrocarbon yield calculations used in the TEA, a lump sum of all fuel-range hydrocarbons is used to set the total GGE yield, based on the products lower heating values (LHVs).

**2.1.5. Area 500 Wastewater Treatment.** The main operation in WWT is anaerobic digestion, similar to the algal process designs described in previous work.[32] The use of an anaerobic digester is important for the life-cycle analysis of algae because of the production of methane coproduct, which, when combusted and sent to a turbine, can offset energy requirements from the grid.[64] This in turn reduces greenhouse gas emissions associated with the

displaced grid electricity.[64] We determined that this additional methane coproduct from waste cyanobacteria biomass was important to the life-cycle analysis and economics, similar to the conclusions drawn from the algae lipid life-cycle analysis and TEA.[28,32] The CP have a low cell biomass concentration, so a set of settling tanks in parallel would be needed to reduce the total volume of the anaerobic digesters.[30] Additionally, gravity thickeners are used to further increase the biomass concentration to 3% solids.[30] The anaerobic digesters operate at 35°C with a 20-day hydraulic retention time.[30] The volatile solids loading rate is 1 kg/day/$m^3$. The gas yield is based on 48.2% carbon degradation, and the composition of the biogas is 67% methane and 33% $CO_2$.[32,65] The AD power demand is set at 0.085 kh/kg total solids.[32,65] Additionally, the heat demand is 0.22 $kWh_{thermal}$/kg total solids.[32,65] The methane-rich biogas for the anaerobic digesters is sent to a gas turbine. The turbine also makes use of concentrated oxygen from Area 200 and fresh air, with operational design specifications based on previous work.[32] Heat is recovered from the flue gas and used for heat demands in other areas of the process. The exhaust turbine flue gas is not recycled to the ethylene cultivation. The liquid effluent from the anaerobic digester contains unreacted solids, nitrogen, water, and phosphorous. With proper solid-liquid separation, the liquid stream with rich nutrients can be recycled to the cultivation system to optimize nutrient consumptions, similar to previous work by Davis et al.[28] When the unreacted solids are removed it is assumed that 20% of the nitrogen, 25% of the water, and 50% of the phosphorous are also removed.[32] An additional 5% of the nitrogen is assumed to be lost to volatilization.[32] The remaining 75% nitrogen, 75% water, and 50% phosphorous are recycled back to the cultivation system. The solid sludge contains a high percentage of nitrogen-rich nutrients (25% of total nitrogen from the anaerobic digester) and is assumed to be sold as a coproduct for fertilizer.[32]

**2.1.6. Area 600 Utilities.** Area 600 facilitates overall energy, water, and power integration. It includes utilities that relate to each area of the process. It accounts for the total requirement of cooling water, chilled water chemicals, power required for a nitrogen refrigeration unit, total power requirement, process water, and heating requirements if additional heating is required. The nitrogen refrigeration unit is not included in the ethylene recovery by solvent absorption design; however, it is needed when cryogenic distillation is used. The refrigeration system takes nitrogen and compresses it to create a high-temperature stream, which is then cooled by cooling water and sent through a turbine to further reduce the temperature and pressure. The cooling water system accounts for cooling water chemicals and the power requirement for pumping the water. If additional heating is required, the amount of purchased natural gas is determined for a heater. Process water accounting determines the amount of make-up water required by the process. Finally, power requirements for the system are determined and purchased from the electrical grid.

### 2.2. Process Economic Analysis

The operating expense calculation for the designed facility is based on material and energy balance calculations using Aspen Plus process simulations.[66] Raw material unit costs are based on literature or existing models, summarized in Table 3. Major raw materials for each area include carbon dioxide, diammonium phosphate, ammonia, monoethanolamine (MEA), hydrogen, water, cooling tower chemicals, electricity, catalysts, and natural gas. The biosolids containing a high percentage of nitrogen are sold as a coproduct. In addition, the absorption solvent separation method requires recycled lean-oil hydrocarbons from the gasoline product. Raw material prices are shown in Table 3. All costs are inflated to 2011 U.S. dollars using the Plant Cost Index from *Chemical Engineering Magazine*,[67] the Industrial Inorganic Chemical Index from SRI Consulting,[68] and the labor indices provided by the U.S. Department of Labor Bureau of Labor Statistics.[69] Salaries for personnel are inflated from 2002 dollars to 2011 dollars.[69] Sixty percent of the total salaries are added for labor burden, and 2.0% of the total installed capital (TIC) is designated for maintenance (which includes expenses on cleaning).[32] Property insurance and taxes account for 1.5% of the total capital investment (TCI).[32]

**Table 3. Raw Material and Utility Cost.**

| Raw Material | Price ($2011) |
|---|---|
| Carbon Dioxide | $40.00/metric ton[32] |
| Diammonium Phosphate | $724.35/metric ton[32] |
| Ammonia | $755.22/metric ton[32] |
| Hydrogen | $1,507.42/metric ton[70] |
| Water | $0.32/metric ton[70] |
| Cooling Tower Chemicals | $3,671.42/metric ton[70] |
| Natural Gas | $4.74/GJ[70] |
| Waste Disposal Cost | $1.14/metric ton[32] |
| Oligomerization Catalyst | $6.04/kg[55] |
| Hydrotreating Catalyst | $19.00/lb[71] |
| Power | $0.0682/kWh[72,73] |
| Monoethanolamine | $3,198.49/metric ton[74] |
| **Coproduct Credit** | **Price ($2011)** |
| Biosolids Containing Nitrogen | ($533.29/metric ton N) [32] |

Material, energy balance, and flow rate information are used to size equipment and to calculate capital expenses. Equipment is sized based on the Aspen Plus simulation of the material and energy balances. Sources for these equipment costs vary from vendor quotations, prior published NREL design reports,[28,30,32,70,74,75] and internal equipment costing databases. For instance, equipment costs for the covered ponds and wastewater treatment (anaerobic digester) are based on a published analysis for algal biofuel processing.[32] PBR reactor costs are based on a previous publication by Davis et al.[28] The oligomerization reactor is extrapolated from a high-pressure tubular reactor from Dutta et al.[75] Based on patent literature, the oligomerization reactor is scaled based on the calculated gas hourly space velocity from.[52] Some standard process equipment, such as distillation columns, pumps, and tanks, are based on costing software calculations (i.e., Aspen Capital Cost Estimator). For most equipment, scaling factors are applied for variations in the throughput or other key design parameters that vary relative to the basis of the original cost estimates, using standard methodologies as described in the NREL 2002 and 2011 design cases.[70,76] Applying scaling factors using the power law to change equipment to fit new capacity requirements is consistent with previously documented methodologies[70,76] as well as indirect capital expenses, except for the additional economic assumptions shown in Table 4. For conceptual analyses of this type, factored equipment estimates are used to project the total project investment based on the calculation of total capital investment.

The discounted cash flow assumes 40% equity financing with a loan interest at 8% for 10 years. Working capital is assumed to be 5% of the fixed capital investment. The plant depreciation period is set for seven years. The plant is assumed to take three years to construct with a quarter of a year spent on start up.

**Table 4. Additional Economic Assumptions.**[32]

| | Value |
|---|---|
| Operating Days per Year | 330 |
| Land Cost | $3,000/acre |
| Inside Battery Limits (ISBL) | Includes Capital Installed Cost of Areas 200–600 |
| Warehouse Development | 1.0% of ISBL |
| Site Development | 9.0% of ISBL |
| Prorateable Expenses | 10.0% of total direct costs |
| Field Expenses | 10.0% of total direct costs |
| Office Construction Fee | 10.0% of total direct costs |
| Project Contingency | 20.0% of total direct costs |
| Other Costs | 5.0% of total direct costs |

The minimum fuel selling price is the price at which the combined gasoline, diesel, and jet fuel products (translated to net GGE yield) must be sold to reach an internal rate of return of 10% and a net present value of 0 at year 30. For the base case, the covered pond for ethylene production and cryogenic separation for ethylene purification are selected. Several sensitivity cases are developed to compare with the base case for variation of cultivation method or separation technology.

## 3. Results and Discussion

### 3.1. Base Case Economics

The base case techno-economic analysis considers a scenario projecting future midterm goals of ethylene productivity in a location with an average solar irradiance of 6,000 MJ/m$^2$/year and is described in section 2.1. The base case process scenario assumes an ethylene cultivation system of tubular PBRs with an ethylene productivity of 7.2 g/m$^2$/day (398 mg/L/day), whereas a comparative sensitivity case instead considers a cultivation system of covered ponds with an ethylene productivity of 7.2 g/m$^2$/day in section 3.2. The areal productivity per square meter of solar radiation given in g/m$^2$/day is set to be consistent with standard productivity rates as typically viewed for photosynthetic organisms such as algae or cyanobacteria.[32] This productivity is a midterm research target, not a theoretical limit. It is important to note that this pre-commercial technology has not yet been demonstrated at appreciable scales, thus the analysis presented here is conceptual in nature, describing plausible projections for technology scale-up in a hypothetical nth-plant facility. Cryogenic distillation is used in the base case to separate and purify ethylene from gas mixtures, as this technology is more established for large-scale applications than the liquid absorption option described in section 2.1. TEA results for the production of hydrocarbon fuels from this bioethylene process are discussed below with a minimum fuel selling price determined for near-term to long-term projections.

**3.1.1. Capital Cost Distribution.** As described in section 2.2, the capital cost for the equipment is estimated from previous TEAs,[28,32,59,70,74,75,77] literature sources, vendor quotes, and Aspen Process Evaluation software. Figure 5 illustrates the equipment cost for each process section. The total installed equipment cost is $443 MM and the total capital investment is $741 MM. The cultivation system (tubular PBRs) accounts for the largest portion of the capital investment at $369 MM. The oligomerization facility for upgrading ethylene to hydrocarbon fuels represents the second largest capital expense at $33 MM, followed by cryogenic distillation and then utilities and wastewater treatment. The combined cost from the PBRs, cryogenic distillation, and oligomerization contributes to more than 95% of the total direct equipment capital costs.

The sensitivity analysis (section 3.2) considers the cost implications when capital expenses are reduced. Ethylene and subsequent hydrocarbon fuel yields play critical roles in capital cost, and by improving ethylene productivity, the capital cost burden of the cultivation system is reduced. The capital expenses can also benefit from economies of scale.[32]

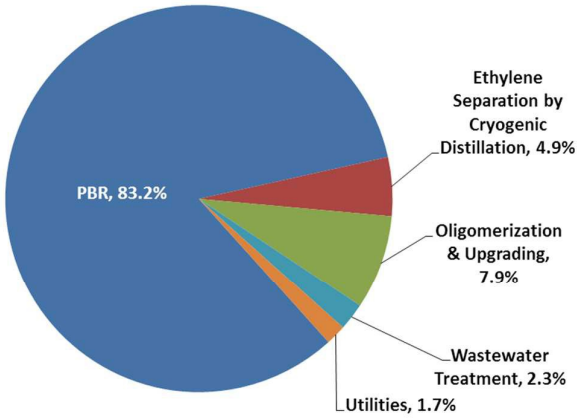


**Figure 5. Capital cost distribution of process unit areas for minimum fuel selling price.**

**3.1.2. Operating Cost Distribution.** Table 5 shows the operating costs for the facility. The costs in Table 5 are broken into six categories including: purchased carbon dioxide, nutrients for the cyanobacteria cell growth and cell maintenance, chemicals for separation and oligomerization, hydrogen, make-up water/water disposal, and purchased electricity.

**Table 5. Operating Expense Distribution.**

| Raw Material | Cost ($MM/yr) |
|---|---|
| Purchased $CO_2$ | 5.8 |
| Nutrients for Cells | 1.3 |
| Chemicals | 0.5 |
| Hydrogen | 0.9 |
| Process Electricity | 18.9 |
| Make-Up Water and Water Disposal | 0.7 |
| **Coproduct Credit** | |
| Sludge Nitrogen Credit | -0.5 |

Additionally, the digestate from the anaerobic digestion of wastewater treatment is credited as a coproduct for its purpose as a fertilizer. The coproduct is credited based on its bioavailable nitrogen content, using the same assumptions as documented in prior work.[32]

The largest operating expense for the facility is purchased electricity, accounting for $18.9 MM per year. On-site power generation from combusting the digester biogas in a gas turbine is not sufficient to power the entire facility; additional grid electricity must be purchased at a rate of $0.0682/kW.[72,73] Electricity consumption attributed to the cryogenic distillation step accounts for more than 90% of the total power consumption, although the estimated capital expense of cryogenic distillation is less than 5% of



 

the total capital. The second largest operating expense is purchasing carbon dioxide for biomass and ethylene production. The carbon dioxide is assumed to be sourced from a flue gas carbon capture operation off site, and is delivered in concentrated form at $40/metric ton.[28]

**3.1.3. Minimum Fuel Selling Price.** For the design basis of 10 MMGGE/yr hydrocarbon fuel production rate, the resulting MFSP with a 10% internal rate of return is $15.07/GGE. Figure 6 shows the total cost contribution associated with each process area, with consideration for capital expense, raw material cost, process electricity, wastewater treatment, and fixed costs.

The ethylene production step using the PBRs accounts for more than 70% of the total MFSP owing to the high capital costs of the PBRs. Cryogenic distillation for purification of ethylene is the second largest cost contributor, driven by purchased electricity for this power-intensive operation. Although capital expenses for converting ethylene to hydrocarbon (oligomerization and hydrotreating reactor systems) are also significant, accounting for 8% of the total MFSP, these technologies are mature and do not represent major cost drivers for the overall process. The cyanobacterial biomass is harvested from the PBRs every 60 days allowing for 2% of the PBRs to be drained and harvested each day. The PBR effluent is assumed subject to gravity thickeners to concentrate the feed material to the wastewater treatment (anaerobic digestion) system to reduce the total volume of the anaerobic digesters.[30] This gravity settling assumes that cyanobacteria will be able to settle similar to some strains of algae.[30] The total capital cost of the gravity thickeners accounts for 5% of the capital cost in the wastewater treatment process area, while the anaerobic digestion units account for 52% of the wastewater treatment cost. The remaining cost in the wastewater treatment area is attributed to a power-generating turbine. Several sensitivity scenarios are considered for their impact on process economics, including use of a covered pond design, a different ethylene separation technology, or different ways to optimize wastewater treatment capacity.

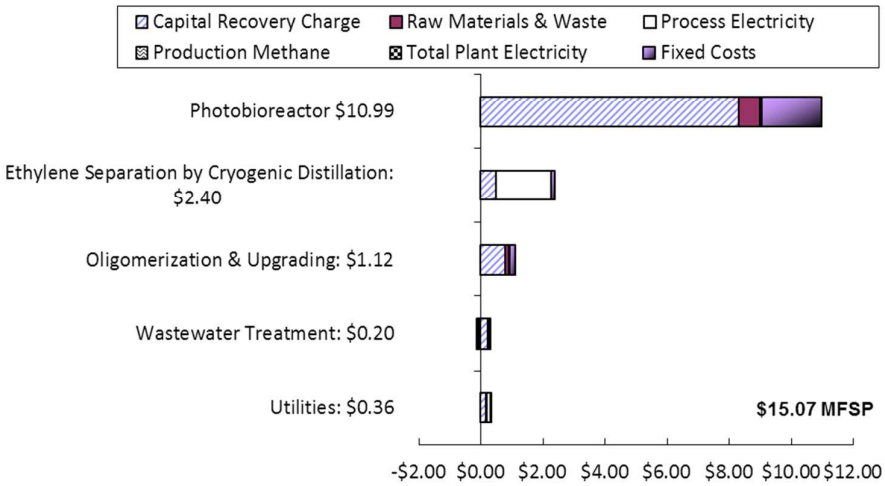


**Figure 6. Cost contribution for each process area to the overall MFSP.**

### 3.2. Sensitivity Analysis

Once key cost drivers are found sensitivity variables are selected to determine the degree the change the variable has on the MFSP. During the sensitivity analysis the plant fuel production is maintained at 10 MMGGE/year, thus the facility footprint is subject to change.

**3.2.1. Single-Point Sensitivity.** A single-point sensitivity analysis uses reasonable minima and maxima for a chosen variable while holding all other factors constant to understand and quantify the resulting cost impact on overall MFSP. Reasonable minima and maxima for each variable are chosen with recommendations from researchers as well as from engineering judgements. Figure 7 shows the single-point sensitivity as a tornado diagram where the variables are sorted based on largest to smallest impact on the MFSP. The variables considered can be classified into four groups: (1) parameters that influence the capital equipment costs, (2) operating cost variations, (3) the turnover time of the cultivation system (the days the system is online before purging the biomass), and (4) ethylene productivity. The type of cultivation system, the TCI, adding a coating to reduce PBR permeability, the clean-in-place system, and the ethylene separation method are capital equipment variables. The ethylene loss due to PBR permeability, $CO_2$ cost, cost of land, oligomerization catalyst cost, coproduct credit value and if the separation operates within the flammability zone are variables that mainly affect the operating costs. Additional discussion on operation within the flammability zone is included in the process design and sensitivity analysis. The ethylene productivity is affected by several variables, such as the quantum requirement, total energy used for ethylene production, photon transmission efficiency, and location with its corresponding full spectrum solar energy. Finally, the turnover time for the cultivation PBRs to purge into the wastewater treatment can affect the required volumetric throughput and equipment capacity of the wastewater treatment area.

One use of single-point sensitivity analysis is to understand uncertainties of the base case economics. For example, although cleaning for the PBR is assumed part of the maintenance cost, additional effective but potentially expensive cleaning techniques include high liquid velocities, mechanical agitation, periodic draining, and refilling the reactor, manual scraping, using glass or plastic particles to scour the side of the reactor, [78] or using chemicals after PBR harvesting. Another strategy is to develop

reactors with super-hydrophobic coating, in order to prevent fouling and eliminate cleaning cost. If we consider using recoverable polyethylene particles (costed at $1,700/metric ton[79] and assumed 1% of the volume of the PBRs) as the clean-in-place (CIP) mechanism for the tubular PBRs, the cost impact of the CIP is pretty small as shown in Figure 7and assumed 1% of the volume of the PBRs) as the clean-in-place (CIP) mechanism for the tubular PBRs,[80] the cost impact of the CIP is pretty small as shown in Figure 7.

Two sensitivities consider the uncertainty of ethylene permeability through the cultivation material. The plastic material of the cultivation system could be permeable to ethylene and specific material testing and safety considerations would be required for each proposed cultivation system in the future. The ethylene loss due to possible PBR permeability is calculated as 12% of the total ethylene produced (see supplementary information for additional information). Permeability can be counteracted with coatings on the PBR and CP liner. These coating have been used in other algae PBR technologies. For example, Algenol has special additives and coating on their PBRs to optimize performance.[81,82] Some recent research on coatings include monolayer graphene, which is impermeable to all gasses and liquids, and at 30 nm thickness are optically transparent.[83] A capital cost is added as a sensitivity case for coating the PBR in a non-permeable material. Because ethylene permeability is not part of the base case it is not considered for the CP sensitivity options, however CP with LDPE could be more permeable to ethylene than PBRs and could pose both a negative effect on the economics due to reduced yields as well as require additional safety considerations. Additional sensitivities include: variation of the oligomerization catalyst cost from $6.04/kg (2011$)[55] to $23.50/kg (2011$)[84], no coproduct credit, varying the TCI.

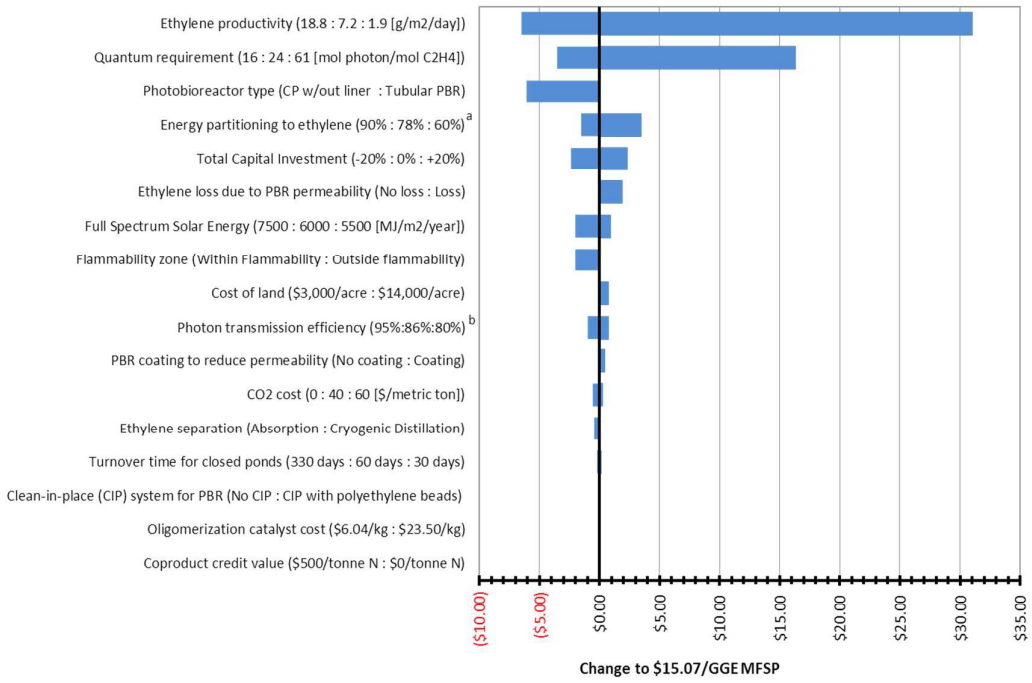


**Figure 7. Single-point sensitivity analysis.** [a.] Energy partitioning to ethylene is the percent of energy that goes to ethylene creation out of the 10.8% of the total solar irradiance that is available for ethylene and biomass production. [b.] The photon transmission efficiency relates to the percent of photons that are transmitted through the closed pond liners into the media.

The ethylene productivity has the most significant impact on cost, as shown in Figure 7, because total production yield and capital cost burden for the capital-intensive cultivation step is dependent on the achievable productivity. Production yield changes the total cultivation system area required to produce 10 MMGGE of hydrocarbon fuels, which can impact cost significantly. The metabolic pathway quantum requirement for ethylene production also makes a significant impact on the overall cost relative to other variables studied here. A quantum requirement of 61 mol photons/mol ethylene (equivalent to 30.5 mol photons/mol $CO_2$ converted)[20,22] results in much lower ethylene productivity and translates to an increase of $16.28/GGE compared to the base case assuming 24 mol photons/mol ethylene (12 mol photons/mol $CO_2$ converted).[18] This finding shows that it is important to determine the solar quantum requirement and understand its limitations, for a low-cost ethylene metabolic pathway. It is also economically beneficial to improve ethylene productivity by improving energy partitioning to ethylene (e.g., by diverting more carbon to products rather than to cell biomass)

The MFSP decreases by $6.10/GGE if the PBRs are replaced with a covered pond design with no liners. Other options for PBRs, such as hanging bags or immobilized cultures, are being studied extensively in literature.[27,85-87] Such alternative cultivation systems may improve economics relative to the costly tubular PBR design considered here. In any case, the design for the cultivation step is likely to be a critical element in ensuring reliable operability, both based on structural integrity and avoiding contamination; such considerations are beyond the conceptual nature of this analysis, but would require more detailed engineering studies and prototype designs to demonstrate. A significant decrease in MFSP may also be



 

realized if the ethylene separation can cross or occur within the flammability zone for a given mixture of ethylene and oxygen (although additional safety precautions would need to be incorporated if such a separation is possible, which is not accounted for here). Although the two separation methods had little effect on the MFSP, additional technologies should be considered to reduce the power demand for separation. Other variables (cost of land, photon transmission efficiency, a PBR coating to reduce permeability, $CO_2$ cost, ethylene separation method,, turnover time, CIP cleaning, oligomerization catalyst cost, and coproduct credit value) individually impact the MFSP by ≤$1.00/GGE, although taken cumulatively could still add up to significant impacts.

Although there is not much economic benefit by switching to solvent absorption as shown in Figure 7, both cases involve separations that dilute the ethylene with air to remain outside the flammability zone. If the separations are able to work within or cross through the flammability zone then the MFSP may be decreased significantly. However, if additional capital costs are related to equipment that can work within the flammability zone the MFSP could increase. This promotes future work on looking into the economics of a more robustly engineered separation system to operate in the flammability zone practically.

**3.2.2. Multiple-Point Sensitivity Analysis.** A multiple-point sensitivity analysis was conducted to show cost comparisons with a combination of two or more process variables. Combinations of cultivation options (tubular PBRs and covered ponds) and ethylene purification options (cryogenic and absorption separation) are compared in Figure 8. The process scenario using covered ponds and absorption separation technology results in the lowest MFSP compared to the others studied. Other separation technologies, such as membranes or solid pressure swing adsorption, may be additional scenarios worth considering. Further research on the development of gas separation technology for this application will be an important area for further reducing cost, similar to improving productivity and alternative PBR designs.

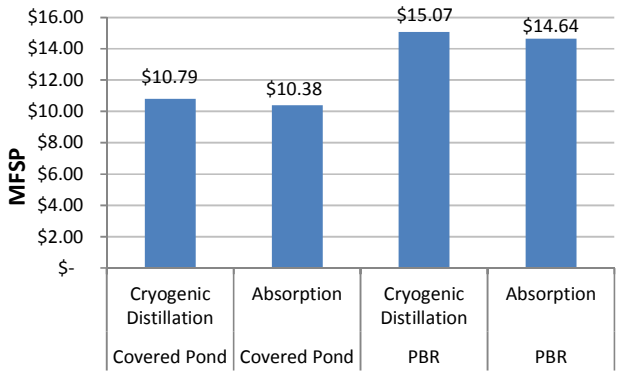


**Figure 8. Multiple-point sensitivity analysis.**

**3.2.3. Cost Prospective for Future Research Directions**

Three scenarios are illustrated in Figure 9 indicating near-term, midterm (base case), and long-term projections by combining several key variables used in the study to project the cost potentials for this technology pathway. This analysis suggests a potential long-term goal is plausible at an estimated $5.36/GGE for high growth (18.8 g/m$^2$/day, 16% of total solar energy to cell biomass and ethylene with 90% of this energy partitioned to ethylene and 10% to cell biomass, plus an assumed 16 quantum requirement), with a near-term projection estimated at $28.66/GGE for low growth (3.2 g/m$^2$/day, 11% of total solar energy to cell biomass and ethylene with 75% of this energy partitioning to ethylene, plus 48 quantum requirement for ethylene).

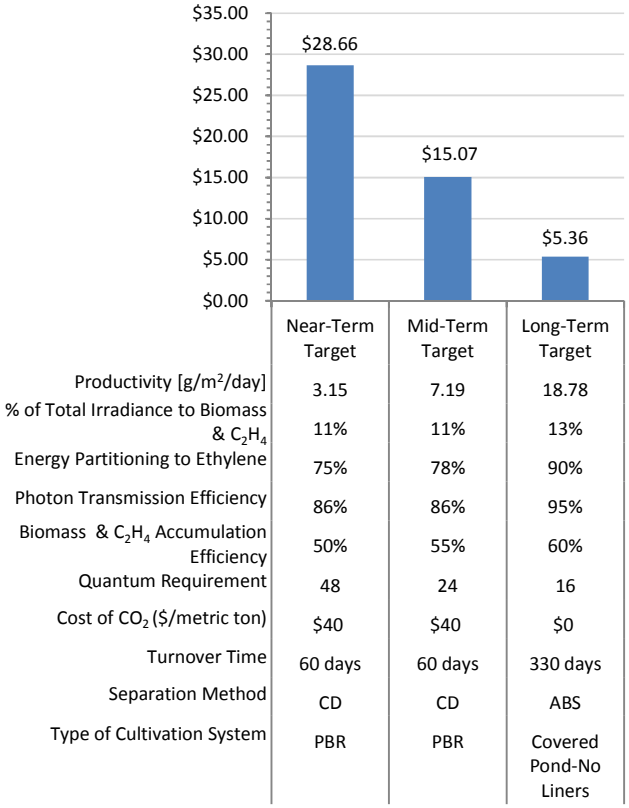


| | Near-Term Target | Mid-Term Target | Long-Term Target |
|---|---|---|---|
| Productivity [g/m$^2$/day] | 3.15 | 7.19 | 18.78 |
| % of Total Irradiance to Biomass & $C_2H_4$ | 11% | 11% | 13% |
| Energy Partitioning to Ethylene | 75% | 78% | 90% |
| Photon Transmission Efficiency | 86% | 86% | 95% |
| Biomass & $C_2H_4$ Accumulation Efficiency | 50% | 55% | 60% |
| Quantum Requirement | 48 | 24 | 16 |
| Cost of $CO_2$ ($/metric ton) | $40 | $40 | $0 |
| Turnover Time | 60 days | 60 days | 330 days |
| Separation Method | CD | CD | ABS |
| Type of Cultivation System | PBR | PBR | Covered Pond-No Liners |

**Figure 9. MFSP for prospective case scenarios.** CD is cryogenic distillation, and ABS stands for absorption separation.

Three parallel research approaches to increase productivity and energy partitioning to ethylene could be pursued to achieve the longer-term projections. First, the limiting factor for ethylene production has been the levels of ethylene-forming enzyme[3] and its substrate alpha ketoglutarate; therefore, synthetic biology tools, such as an optimized gene copy number, promoter, and ribosome-binding site, should be applied to increase ethylene-forming enzyme expression levels and substrate supply. Second, current metabolic pathways leading to ethylene production are not carbon efficient[11] and the utilization of energy-efficient metabolic pathways such as the phosphoketolase reaction[88] could be explored. Third, the EFE reaction may consist of two sub-reactions from a common intermediate—one yields ethylene and another does not—therefore enzyme engineering could maximize the ethylene-producing sub-reaction and minimize the non-productive sub-reaction.[11] Besides carbon partition rate improvements, the ethylene production rate could be further increased by enhancement of the photosynthetic carbon fixation rate. Light harvesting could be improved by expanding the photosynthetically active solar spectrum via pigments that absorb red and infrared light. It has also been observed that there is increased $CO_2$ fixation rates in ethylene producing strains, suggesting that ethylene production triggers a natural regulatory mechanism in *Synechocystis* to increase photosynthesis,[14] with increased carbon fixation from both ribulose-1,5-bisphosphate

carboxylase/oxygenase (RuBisCO) and phosphoenolpyruvate (PEP) carboxylase.

Understanding this regulatory mechanism could lead to additional increases in carbon fixation rates and ethylene productivity. In the meantime, the quantum requirement should be experimentally determined and improved by pathway and enzyme engineering as mentioned above. The durability of the culture should be improved from the demonstrated 71 days to the best case of close to a year with further demonstration. The photon transmission efficiency could be increased by using materials for the PBR that allow for a greater light penetration. In addition, supplemental energy inputs, such as a light-concentrating device, supplemental illumination, and biomass-derived sugars, could be considered to further increase ethylene productivity, although they may also increase the process costs. Progress has been made on engineering *Synechocystis* to convert xylose and glucose to ethylene at higher productivity than photosynthesis alone.[10] Mixotrophic conversion of low-cost organic feedstocks as well as $CO_2$ could support ethylene productivity beyond what's considered best case productivity at about 11% solar energy input[23] but at the cost of utilizing an additional feedstock. Other more advanced PBR systems, such as immobilized cells [87], could be considered in the future with potentials of improving productivity to achieve long-term cost projections.

In all, Figure 9 suggests that to achieve economic viability, improvements to cell biology (productivity and energy partitioning to ethylene) and system engineering (designing a cost-effective closed cultivation system, separation technologies, and wastewater treatment technologies) will be required together. To further reduce cost below $5.36/GGE (equivalent to $225/barrel oil), further improvements to photosynthetic efficiency and cell biology would be required, as well as additional energy input such as biomass sugars. Utilization of biomass sugars has been explored to enhance ethylene productivity[10] and may be considered in future TEAs. Today's crude oil price is $45/barrel (accessed on July 20th, 2016, http://www.bloomberg.com/energy), which is equivalent to MFSP of $1.07/GGE (assuming each barrel is 42 gallon gasoline equivalent). Thus, development of lower cost cultivation systems may further reduce MFSP to be cost comparable with fossil derived fuel costs, along with advances in other process and separation technologies.

## 4. Conclusion

Techno-economic analysis was performed for a new technology pathway to photosynthetically produce ethylene using cyanobacteria, $CO_2$, and sunlight. For a process conversion facility with an annual production rate of 10 MMGGE hydrocarbon fuel, the minimum selling price was projected at $15.07/GGE as a midterm projection, with near-term cost potentials at $28.66/GGE and long-term potentials at $5.36/GGE. The ethylene productivity from photosynthesis was identified as the most critical variable for cost reduction as it combines the effects from the quantum requirement, energy partitioning, biomass and ethylene accumulation efficiency (cost of living for the cell), photon transmission efficiency, and location. Therefore research priorities should focus on understanding the quantum requirement of ethylene synthesis, maximizing energy partitioning to ethylene, minimizing the energy cost of living for cells, and increasing the photon transmission efficiency. Separating ethylene within the flammability zone can also improve costs and the net energy ratio. This analysis shows that a cost reduction for the long-term projection scenario can be achieved through synergistic improvements in productivity, reactor design, and separation technologies.

## Acknowledgements

The authors wish to acknowledge the following funding sources:
U.S. Department of Energy, (1) Office of Energy Efficiency and Renewable Energy, Bioenergy Technologies Office (JM, LT, RD, JU, JY), and (2) Advanced Research Projects Agency-Energy (ARPA_E) (NV, LA). We also thank Mary Biddy, Maria Ghirardi, Pin-Ching Maness, and Philip Pienkos for critical readings of the manuscript.

## References

1. A. Lundgren and T. Hjertberg, in *Surfactants from Renewable Resources*, eds. M. Kjellin and I. Johansson, John Wiley & Sons, Chichester, U.K., 2010, pp. 111-126.
2. SRI Consulting, *Chemical economic handbook marketing research report: ethylene*, SRI International, Englewood, CO, USA, 2011.
3. J. Ungerer, L. Tao, M. Davis, M. Ghirardi, P. C. Maness and J. P. Yu, *Energ Environ Sci*, 2012, **5**, 8998-9006.
4. A. Inkpen and M. H. Moffett, in *Global oil and gas industry - management, strategy and finance*, ed. M. Patterson, PennWell, Tulsa, 2011, pp. 506-534.
5. V. N. Ipatieff and B. B. Corson, *Industrial & Engineering Chemistry*, 1936, **28**, 860-863.
6. Braskem, I'm green polyethylene, http://www.braskem.com.br/site.aspx/Im-greenTM-Polyethylene, (accessed July 23, 2015).
7. H. Weingart, H. Ullrich, K. Geider and B. Volksch, *Phytopathology*, 2001, **91**, 511-518.
8. P. R. Johnson and J. R. Ecker, *Annual review of genetics*, 1998, **32**, 227-254.
9. K. L. Wang, H. Li and J. R. Ecker, *The Plant cell*, 2002, **14 Suppl**, S131-151.
10. T. C. Lee, W. Xiong, T. Paddock, D. Carrieri, I. F. Chang, H. F. Chiu, J. Ungerer, S. H. H. Juo, P. C. Maness and J. P. Yu, *Metab Eng*, 2015, **30**, 179-189.
11. C. Eckert, W. Xu, W. Xiong, S. Lynch, J. Ungerer, L. Tao, R. Gill, P. C. Maness and J. Yu, *Biotechnology for biofuels*, 2014, **7**, 33.
12. H. Fukuda, T. Ogawa, M. Tazaki, K. Nagahama, T. Fujiil, S. Tanase and Y. Morino, *Biochemical and Biophysical Research Communications*, 1992, **188**, 483-489.
13. J. Yu and J. Ungerer, Presentation: Photobiological ethylene production in Synechocystis 6803, Washington University, St. Louis, 2013.
14. W. Xiong, J. A. Morgan, J. Ungerer, B. Wang, P.-C. Maness and J. Yu, *Nature Plants*, 2015, **1**, 15053.
15. R. H. Wijffels, O. Kruse and K. J. Hellingwerf, *Current Opinion in Biotechnology*, 2013, **24**, 405-413.
16. S. A. Angermayr, A. G. Rovira and K. J. Hellingwerf, *Trends in biotechnology*, 2015, **33**, 352-361.
17. M. C. Lai and E. I. Lan, *Metabolites*, 2015, **5**, 636-658.
18. D. E. Robertson, S. A. Jacobson, F. Morgan, D. Berry, G. M. Church and N. B. Afeyan, *Photosynth Res*, 2011, **107**, 269-277.
19. T. T. Vu, E. A. Hill, L. A. Kucek, A. E. Konopka, A. S. Beliaev and J. L. Reed, *Biotechnology Journal*, 2013, **8**, 619-630.
20. H. Knoop and R. Steuer, *Frontiers in Bioengineering and Biotechnology*, 2015, **3**, 47.

21. E. I. Lan and J. C. Liao, *Metab Eng*, 2011, **13**, 353-363.
22. J. Kämäräinen, H. Knoop, N. J. Stanford, F. Guerrero, M. K. Akhtar, E.-M. Aro, R. Steuer and P. R. Jones, *Journal of Biotechnology*, 2012, **162**, 67-74.
23. K. Weyer, D. Bush, A. Darzins and B. Willson, *Bioenerg. Res.*, 2010, **3**, 204-213.
24. U.S. Department of Energy, EnergyPlus Weather Data, https://energyplus.net/weather, (accessed July 25, 2016).
25. G. Burgess and J. G. Fernández-Velasco, *International Journal of Hydrogen Energy*, 2007, **32**, 1225-1234.
26. Y. Yu, L. You, D. Liu, W. Hollinshead, Y. Tang and F. Zhang, *Marine Drugs*, 2013, **11**, 2894-2916.
27. G. C. Zittelli, N. Biondi, L. Rodolfi and M. R. Tredici, *Handbook of microalgal culture: applied phycology and biotechnology*, 2013, **2**, 225-266.
28. R. Davis, A. Aden and P. T. Pienkos, *Appl Energ*, 2011, **88**, 3524-3531.
29. A. Sun, R. Davis, M. Starbuck, A. Ben-Amotz, R. Pate and P. T. Pienkos, *Energy*, 2011, **36**, 5169-5179.
30. T. J. Lundquist, I. C. Woertz, N. Quinn and J. R. Benemann, *Energy Biosciences Institute*, 2010, 1.
31. R. Davis, J. Markham, C. Kinchin, N. Grundl, E. Tan and D. Humbird, *Process design and economics for the production of algal biomass: algal biomass production in open pond systems and processing through dewatering for downstream conversion*, Report NREL/TP-5100-64772, National Renewable Energy Laboratory, Golden, CO, 2016.
32. R. Davis, D. Fishman, E. Frank, M. Wigmosta, A. Aden, A. Coleman, P. Pienkos, R. Skaggs, E. Venteris and M. Wang, *Renewable diesel from algal lipids: an integrated baseline for cost, emissions, and resource potential from a harmonized model*, Report NREL/TP-5100-55431, National Renewable Energy Laboratory, Golden, CO, 2012.
33. Q. Béchet, A. Shilton, O. B. Fringer, R. Muñoz and B. Guieysse, *Environmental Science & Technology*, 2010, **44**, 2197-2203.
34. M. G. Zabetakis, *Flammability characteristics of combustible gases and vapors*, Report USBM Bulletin 627, U.S. Bureau of Mines Washington, D.C., 1965.
35. *U.S. Pat.,* 5,859,304, 1999.
36. *US Pat.,* 4,900,347, 1990.
37. *US Pat.,* 6,468,329, 2002.
38. J.-i. Hayashi, H. Mizuta, M. Yamamoto, K. Kusakabe, S. Morooka and S.-H. Suh, *Industrial & Engineering Chemistry Research*, 1996, **35**, 4176-4181.
39. *US Pat.,* 4,923,493, 1990.
40. *US Pat.,* 5,019,143, 1991.
41. *US Pat.,* 2,308,856, 1943.
42. *US Pat.,* 5,546,764, 1996.
43. *US Pat.,* 5,462,583, 1995.
44. *US Pat.,* 2,433,286, 1947.
45. A. Forestière, H. Olivier-Bourbigou and L. Saussine, *Oil & Gas Science and Technology-Revue de l'IFP*, 2009, **64**, 649-667.
46. K. Weissermel and H. J. Arpe, *Industrial organic chemistry*, John Wiley & Sons, New York, NY, 3rd edn., 2008.
47. P. W. N. M. Van Leeuwen, N. D. Clément and M. J. L. Tschan, *Coordination Chemistry Reviews*, 2011, **255**, 1499-1517.
48. S. Aldrett and J. H. Worstell, Improved ethylene oligomerization modeling using Aspentech's Polymers Plus San Francisco, CA, 2003.
49. S. A. Svejda and M. Brookhart, *Organometallics*, 1998, **18**, 65-74.
50. *US Pat.,* 3,663,647, 1972.
51. H. W. Stache, ed., *Anionic surfactants: organic chemistry*, Marcel Dekker, New York, 1995.
52. *US Pat.,* 3,702,345, 1972.
53. D. L. Burdick and W. L. Leffler, *Petrochemicals in Nontechnical Language*, PennWell, 4th edn., 2010.
54. N. P. Cheremisinoff, *Handbook of hazardous chemical properties*, Butterworth-Heinemann, Boston, 2000.
55. Zhejiang Friend Chemical Co., Triethylaluminum, http://www.manufacturer.com/triethylaluminum-products-p6653492, (accessed June, 30, 2016).
56. J. H. SB Jones, C Valkenburg, DJ Stevens, CW Walton, C Kinchin, DC Elliott, S Czernik, *Production of gasoline and diesel from biomass via fast pyrolysis, hydrotreating and hydrocracking: A design case*, Report PNNL-18284, Pacific Northwest National Laboratory Richland, WA, 2009.
57. *US Pat.,* 2011/0288352, 2011.
58. *US Pat.,* 8,193,402B2, 2012.
59. R. Davis, L. Tao, E. C. Tan, M. J. Biddy, G. Beckham, C. J. Scarlata, J. Jacobson, K. Cafferty, J. Ross, J. Lukas, D. Knorr and P. Schoen, *Process design and economics for the conversion of lignocellulosic biomass to hydrocarbons-dilute-acid and enzymatic deconstruction of biomass to sugars and biological conversion of sugars to hydrocarbons*, Report NREL/TP-5100-60223, National Renewable Energy Laboratory, Golden, CO, 2013.
60. M. Busto, M. E. Lovato, C. R. Vera, K. Shimizu and J. M. Grau, *Appl Catal a-Gen*, 2009, **355**, 123-131.
61. G. E. H. James H. Gary, Mark J. Kaiser, *Petroleum refining, technology and economics*, CRC Press, Boca Raton, FL, 2001.
62. S. V. Konnov, I. I. Ivanova, O. A. Ponomareva and V. I. Zaikovskii, *Micropor Mesopor Mat*, 2012, **164**, 222-231.
63. K. R. Venkatesh, J. Hu, W. Wang, G. D. Holder, J. W. Tierney and I. Wender, *Energ Fuel*, 1996, **10**, 1163-1170.
64. D. L. Sills, V. Paramita, M. J. Franke, M. C. Johnson, T. M. Akabas, C. H. Greene and J. W. Tester, *Environmental Science & Technology*, 2012, **47**, 687-694.
65. R. Davis, C. Kinchin, J. Markham, E. Tan and L. Laurens, *Process design and economics for the conversion of algal biomass to biofuels: algal biomass fractionation to lipid and carbohydrate fuel products*, Report NREL/TP-5100-62368, National Renewable Energy Laboratory, Golden, CO, 2014.
66. AspenPlus™, *Release 7.2, Aspen Technology Inc., Cambridge MA*, 2007.
67. Chemical Engineering Magazine, http://www.chemengonline.com/pci-home, (accessed May 25, 2013).
68. SRI Consulting, in *Chemical Economics Handbook*, Menlo Park, CA. , 2008.
69. Bureau of Labor Statistics Data website, Bureau of Labor Statistics Data website, National employment, hours, and earnings catalog, industry: chemicals and allied products, 1980-2009., http://data.bls.gov/cgi-bin/srgate, (accessed January 1, 2011).
70. D. Humbird, R. Davis, L. Tao, C. Kinchin, D. Hsu, A. Aden, P. Schoen, J. Lukas, B. Olthof, M. Worley, D. Sexton and D. Dudgeon, *Process design and economics for biochemical conversion of lignocellulosic biomass to ethanol: dilute-acid pretreatment and enzymatic hydrolysis of corn stover*, Report NREL/TP-510-47764, National Renewable Energy Laboratory, Golden, CO, 2011.
71. S. Jones, J. Holladay, C. Valkenburg, D. Stevens, C. Walton, C. Kinchin, D. Elliott and S. Czernik, *Production of gasoline and*

*diesel from biomass via fast pyrolysis, hydrotreating and hydrocracking: a design case*, Report PNNL-18284, Pacific Northwest National Laboratory Richland, WA, 2009.
72. U.S. EIA, Electricity wholesale market data, http://www.eia.gov/electricity/wholesale/index.cfm, (accessed July 24, 2013).
73. U.S. EIA, Average retail price of electricity to ultimate customers: Industrial, https://www.eia.gov/electricity/data.cfm#sales, (accessed July 10, 2016).
74. A. Dutta and S. Phillips, *Thermochemical ethanol via direct gasification and mixed alcohol synthesis of lignocellulosic biomass*, Report NREL/TP-510-45913, National Renewable Energy Laboratory, Golden, CO, 2009.
75. M. T. A Dutta, J. Hensley, M. Worley, D. Dudgeon, D. Barton, P. Groenendijk, D. Ferrari, B. Stears, E. M. Searcy, C.T. Wright, J.R. Hess, *Process design and economics for conversion of lignocellulosic biomass to ethanol, thermaochemical pathway by indirect gasification and mixed alcohol synthesis*, Report NREL/TP-5100-51400, National Renewable Energy Laboratory (NREL) Golden, CO, 2011.
76. A. Aden, M. Ruth, K. Ibsen, J. Jechura, K. Neeves, J. Sheehan, B. Wallace, L. Montague, A. Slayton and J. Lukas, *Lignocellulosic biomass to ethanol process design and economics utilizing co-current dilute acid prehydrolysis and enzymatic hydrolysis for corn stover*, Report NREL/TP-510-32438, National Renewable Energy Laboratory, Golden, CO, 2002.
77. SRI Internationl, *Liquid hydrocarbons from synthesis gas*, Report Process Economics Program Report 191A, 1999.
78. B. D. Fernandes, A. Mota, J. A. Teixeira and A. A. Vicente, *Biotechnology Advances*, 2015, **33**, 1228-1245.
79. Platts Global Petrochemical Index, Platts Global Low-Density Polyethylene (LDPE) Price Index, http://www.platts.com/news-feature/2014/petrochemicals/pgpi/ldpe, (accessed July 8, 2016).
80. F. G. Acién, J. M. Fernández, J. J. Magán and E. Molina, *Biotechnology Advances*, 2012, **30**, 1344-1353.
81. BioRefineries Blog, The pilot-scale intergrated biorefinery of Algenol, https://biorrefineria.blogspot.com/2016/05/the-pilot-scale-algae-integrated-biorefinery-algenol.html, (accessed July 10, 2016).
82. K. Spall, F. Jochem, B. McCool and R. Chance, presented in part at the Florida Energy Systems Consortium University of Florida, 2011.
83. Y. Su, V. Kravets, S. Wong, J. Waters, A. Geim and R. Nair, *Nature communications*, 2014, **5**.
84. D. B. Malpass, in *Handbook of Transition Metal Polymerization Catalysts*, John Wiley & Sons, Inc., Online, 2010, DOI: 10.1002/9780470504437.ch1, pp. 1-28.
85. B. Bharathiraja, M. Chakravarthy, R. Ranjith Kumar, D. Yogendran, D. Yuvaraj, J. Jayamuthunagai, R. Praveen Kumar and S. Palani, *Renewable and Sustainable Energy Reviews*, 2015, **47**, 634-653.
86. S. A. Markov, E. S. Protasov, V. A. Bybin, E. R. Eivazova and D. I. Stom, *International Journal of Hydrogen Energy*, 2015, **40**, 4752-4757.
87. L. Katarzyna, G. Sai and O. A. Singh, *Renewable and Sustainable Energy Reviews*, 2015, **42**, 1418-1427.
88. W. Xiong, T.-C. Lee, S. Rommelfanger, E. Gjersing, M. Cano, P.-C. Maness, M. Ghirardi and J. Yu, *Nature plants*, 2015, **2**, 15187.